Wideband Measurements of Angle and Delay Dispersion for Outdoor and Indoor Peer-to-Peer Radio Channels at 1920 MHz

Gregory D. Durgin, *Member, IEEE*, Vikas Kukshya, and Theodore S. Rappaport, *Fellow, IEEE*

***Abstract*—This paper presents spatio-temporal measurements for the *peer-to-peer* radio channel at a center frequency of 1920 MHz with 140 MHz of radio-frequency bandwidth. The measurements were taken using a spread-spectrum channel sounder and an automated spatial probing system that uses precise computer-controlled positioning and orientation of omnidirectional and directional (30° beamwidth) antennas to measure both the angles-of-arrival and time-delays of multipath components. Transmitter-receiver configurations included six outdoor-to-outdoor cross-campus locations at Virginia Polytechnic Institute and State University (17–219 ns rms delay spread, 0.36–0.91 angular spread—using the unitless definition of angular spread defined in [1]), three outdoor-to-indoor locations (27–34 ns rms delay spread, 0.78–0.98 angular spread), and three indoor-to-indoor locations (29–45 ns rms delay spread, 0.73–0.90 angular spread). The paper also quantitatively describes a trend that shows how angular spread increases with increasing delay spread.**

***Index Terms*—Angle of arrival, fading channels, mobile communications, multipath channels, peer-to-peer, propagation.**

I. Introduction

In THE coming age of high wireless data demand and increased frequency congestion, technologies involving wideband modulation schemes [2], smart antennas [3], and space-time coding [4], [5] promise to squeeze every drop of capacity out of a wireless data link. Unfortunately, these new technologies have grown at a rate that exceeds our general knowledge of the spatio-temporal wireless channel. Without sufficient knowledge of the channel, the performance of new spatial and wideband signaling techniques is impossible to gauge for a particular radio environment.

This paper presents the results of a wideband, *peer-to-peer* channel measurement campaign at a carrier frequency of 1920 MHz conducted on the campus of Virginia Polytechnic Institute and State University (Virginia Tech) in November of 1999. In the peer-to-peer configuration, both transmitter and antennas are positioned at a height of roughly 1.5 m above ground (head-level). This position is common for portable, handheld communication devices that may operate in mobile ad-hoc networks. Future applications for these peer-to-peer, mobile ad-hoc networks include communications between students, soldiers, businessmen, or emergency rescue workers.

A. Contribution of This Work

In this paper, peer-to-peer channel statistics for 12 local areas are derived from over 2500 ultrawideband power delay profile (PDP) snapshots taken with a spread-spectrum sliding correlator channel sounder with 140 MHz of radio frequency bandwidth. This measurement campaign is unique and valuable for the following reasons.

- Joint statistics involving multipath delay dispersion and angle dispersion have been measured at each local area.
- A variety of transmitter-receiver configurations—outdoor-to-outdoor, outdoor-to-indoor, and indoor-to-indoor—were measured.
- This paper uses a combination of directional antennas and mechanical positioning, similar to the spatial channel sounding techniques presented first in [6], [7], as opposed to antenna arrays. This spatial channel sounding technique facilitates wideband spatial channel sounding at potentially any carrier frequency in the UHF, microwave, or mm-wave bands.
- The spatial channel parameters are calculated in terms of multipath *shape factors*, one of the first such applications of the theory described in [8].

The results should prove valuable to designers of high-capacity wireless modems and future joint spatio-temporal channel measurement campaigns.

B. Comparison to Other Measurement Campaigns in the Literature

The first documented attempt to measure both angle-of-arrival and time-delay of mobile radio multipath components was made by the Japanese researchers Ikegami and Yoshida [9]. More recent spatio-temporal results have been published in [10] and [11], although these research papers measure only a few locations and are meant largely to prove new techniques and concepts in spatio-temporal channel measurement. Pedersen, *et al.* have also published delay and azimuthal dispersion results for base station antennas in urban areas [12]. Overall, however, little

Manuscript received November 1, 2001; revised April 4, 2002. This work was supported by ITT Defense and Electronics, Incorporated and a Bradley Fellowship in Electrical and Computer Engineering from Virginia Polytechnic Institute and State University, Blacksburg, VA 24061-0202 USA. This paper was presented in part at the IEEE Antennas and Propagation Society Symposium, Boston, MA, July 8–3, 2001.

G. D. Durgin was with Morinaga Laboratory, Osaka University, Osaka 567-0047, Japan. He is now at 1520 Village Green Dr., Woodbine, MD 21797 USA (gdurgin@vt.edu).

V. Kukshya is with the HRL Laboratories, LLC, Malibu, CA 90265 USA (vkukshya@hrl.com).

T. S. Rappaport is with the Wireless Networking and Communications Group, University of Texas-Austin, Austin, TX 78712 USA (wireless@mail.utexas.edu).

Digital Object Identifier 10.1109/TAP.2003.811494

is known about the joint spatio-temporal characteristics for most types of radio channels.

While the bands around 1920 MHz have been measured extensively for cellular and personal communication system (PCS) applications, measurements previously reported in the literature involve transmitters at least five meters above the ground—still much higher than in a genuine peer-to-peer environment. The range of peer-to-peer outdoor delay spreads presented in this paper is much lower than typical delay spreads measured for mobile radio macrocells (2–3 μs, [13]) and is more similar to PCS microcell measurements (mean of 137 ns [14]). This is expected since peer-to-peer communications are much more lossy than macrocellular configurations; both the transmitter and the receiver are close to the ground, buried within building, foliage, and terrain clutter.

Our campaign finds a similar range of outdoor root mean square (rms) delay spreads (17 to 219 ns) to those reported by Patwari, *et al.* in [15] (25 to 333 ns) and those described by Erceg, *et al.* in [16] (50 to 175 ns, omnidirectional data taken in a cluttered Illinois environment). Unlike the measurements in [15], this paper directly measures the angles-of-arrival of multipath components. Thus, delay dispersion (Section III-A), angle dispersion (Section III-B), and joint angle-delay statistics (Section III-C) are presented for all indoor and outdoor measurement locations.

For indoor receiver locations, our measurements exhibit much lower rms (delay spreads (27–45 ns) than the outdoor locations. Devasirvatham, *et al.* corroborates this result in an exhaustive indoor measurement campaign that shows delay spreads are less than 100 ns for indoor office buildings [17]. Woodward, *et al.* present a set of measurements at 2.4 GHz that record angle-of-arrival and delay statistics for outdoor-to-indoor configurations. In an urban building, they show low values of rms delay spread (mean 37 ns) but high values of rms azimuth angle spread (89° which is 86% of the rms azimuth spread for the uniform Clarke model) [18]. This compares favorably to our range of outdoor-to-indoor delay spreads of 27–44 ns and our angle spread values which show angles-of-arrival spread out from 73%–98% of the uniform Clarke model.

II. Overview of Measurement Campaign

This section provides a general overview of the measured locations, channel sounding hardware, and measurement technique used throughout the campaign.

A. Measured Locations

The measurement campaign was performed during November of 1999 on the campus of Virginia Tech. A total of 12 locations were measured during this campaign using the peer-to-peer configuration of transmitter and receiver antennas (both set at a height of 1.5 m above ground).

The first set of six measurements were outdoor-to-outdoor locations which emphasized long-distance, obstructed links with transmitter-receiver (TR) separation distances between 240 and 910 m. The signal had to propagate over irregular campus terrain which included hills, multi-story buildings, and leafless trees.

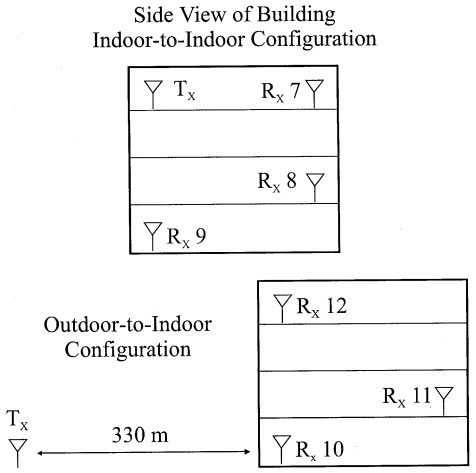

Fig. 1. Transmitter-receiver configurations for the six local areas measured indoors.

Then, three indoor-to-indoor locations were measured inside a four-story modern office building (Durham Hall on the Virginia Tech campus) with interior walls made from either cinderblocks or drywall. The same transmitter—placed inside a fourth-floor office—was used for all three indoor-to-indoor measurements. One receiver location was measured on the same floor as the transmitter, on the opposite side of the building. Another receiver location was measured on the ground floor, on the same side of the building as the transmitter. A third location was measured on a different floor than the transmitter *and* on the opposite side of the building.

Finally, three outdoor-to-indoor locations were measured using a transmitter placed 330 m away from the four-story office building. The exterior of this office building is a combination of glass, concrete, and stone masonry. One receiver location was measured on the ground floor, on the same side of the building as the transmitter. Another receiver location was measured on the fourth floor, also on the same side of the building as the transmitter. A third location on the back side of the building was measured as well. A graphical summary of the six indoor local area configurations may be found in Fig 1.

B. Channel Sounding Hardware

A spread spectrum sliding correlator approach was used to sound the channel (see [19] for a description). A transmitted carrier frequency of 1920 MHz was used throughout the campaign. The transmitted spread spectrum signal had a radio frequency (RF) bandwidth of 200 MHz, allowing for theoretical resolution of multipath with as little as 10 ns of propagation delay. In practice, the resolution was slightly worse since we filtered the signal with a 140 MHz passband filter to remain within our allowed band of 1850–1990 MHz. Since this is an active PCS band in the U.S., the interference rejection capability of the sliding correlator was particularly useful.

In order to send the channel sounding signal through the lossy peer-to-peer environment, the transmitter used a 20-watt wideband RF amplifier. Special precautions were taken to control the temperature of the RF hardware and to limit human RF exposure. Back-to-back system calibrations were performed on the

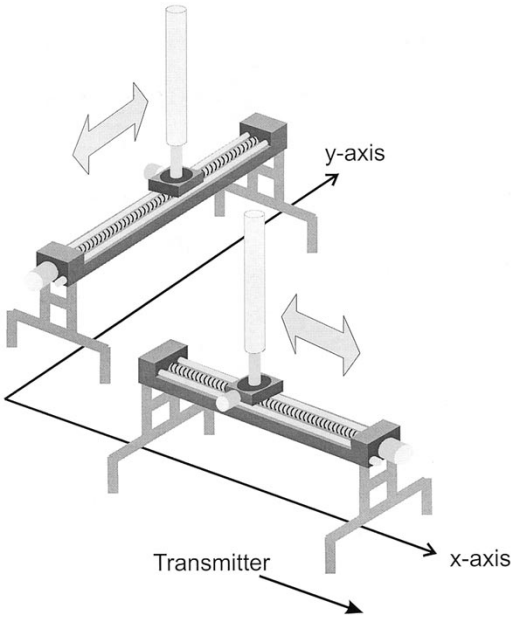

Fig. 2. In a local area, power delay profiles are measured along two orthogonal linear tracks using an omnidirectional antenna.

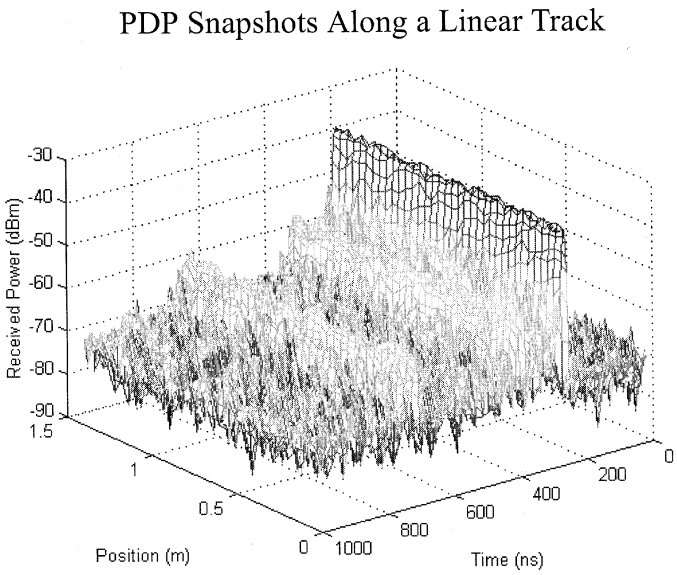

Fig. 3. Series of PDP snapshots along a track, measured with an omnidirectional receiver antenna.

transmitter and receiver units at the beginning and the end of each measurement day to ensure system stability.

C. Automated Antenna Positioning

All measurements used a precise automated positioning system to place the receiver antenna along a linear track and, for a directional antenna, to orient the antenna with respect to azimuth. The antenna platform is positioned using stepper motors that drive a rotating table and a long serpentine-drive track. The positioning error for placement along the track is ± 10 μm and for rotation about an axis it is $\pm 0.01^{\circ}$.

A laptop computer simultaneously coordinated the movement and rotation of the receiver antenna and the data acquisition from the channel sounder. This system was used to take two types of measurement sequences: *track measurements* and *rotational measurements*.

Track Measurements: For the track measurement sequence, an omnidirectional antenna is mounted atop the positioning table. Two linear track measurements are performed, each using different track orientations. The first orientation aligns the track along an axis (referred to as the x axis) directed along the line connecting the transmitter to the receiver. The second orientation aligns the track along an axis (referred to as the y axis) transverse to the direction of the transmitter location. The orientations are depicted in Fig. 2. For each linear track measurement, snapshots of the channel PDP are taken along the length of the measurement track (about nine wavelengths at 1920 MHz). Each PDP snapshot is spaced 0.25 wavelengths apart, producing a total of 36 snapshots per linear track measurement. Thus, a measurement along two orthogonal tracks produces a total of 72 PDP snapshots. An example of collected PDPs as a function of position is shown in Fig. 3.

Rotational Measurements: The second measurement sequence at a location is a rotational measurement using a directional antenna. PDP snapshots are recorded from the channel sounder as the test antenna is rotated in steps across the entire horizon in evenly-spaced 10° increments. Thus, a single sweep in the rotational measurement results in a total of 36 PDP snapshots. The antenna platform is then moved along the track by 2.67 wavelengths (0.42 meters) and another series of 36 rotational PDP snapshots are recorded. This procedure is repeated until a fourth rotational measurement is made. Fig. 4 illustrates this sequence of measurements. In all, the rotational measurement sequence results in a total of 144 PDP snapshots. An example of collected PDPs as a function of azimuth orientation is shown in Fig. 5.

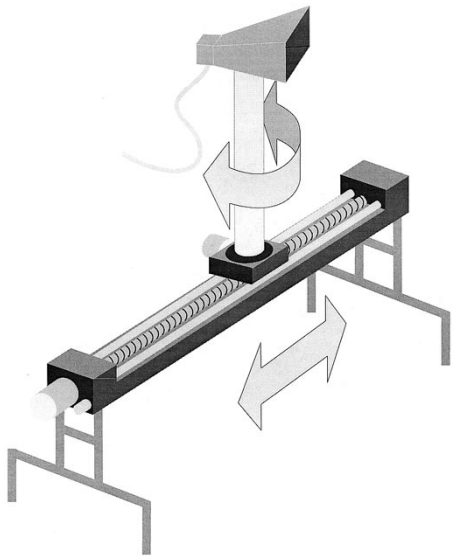

Fig. 4. In a local area, power delay profiles are measured by spatially averaging angular sweeps with a directional antenna.

D. Antenna Specifications

All antennas used during this campaign had sufficient bandwidth over the 1850–1990 MHz frequencies to transmit and receive the wideband spread spectrum signal without distortion in

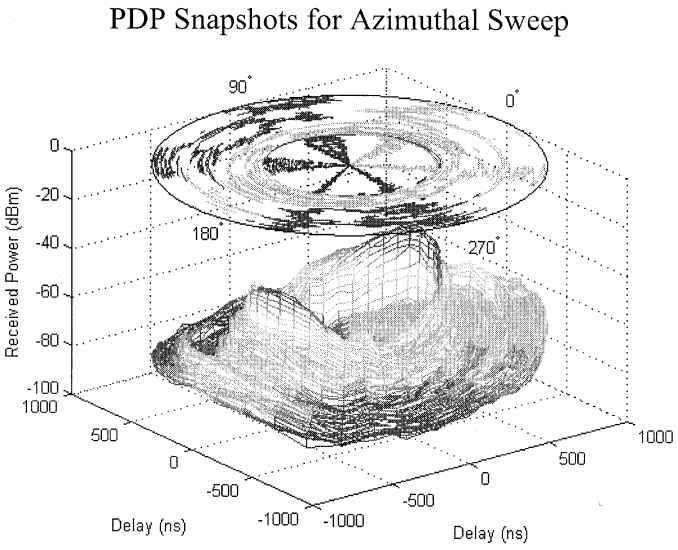

Fig. 5. Local area angle-delay spectrum (ADS) as measured from a set of rotational measurements.

space or time delay (by a frequency-varying antenna pattern or impedance/efficiency). An omnidirectional PCS base station antenna made by Andrew Corporation was used at the transmitter. This antenna had a gain of 8 dBi along the horizon—the direction of peak gain for the elevation pattern. This same type of antenna was also used at the receiver for the track measurements.

The rotational measurements used a directional horn antenna. The horn antenna had a gain of 15 dBi and a half-power beamwidth of 30°. All antennas used at the receivers are elevated to 1.5 m height using poly-vinyl chloride masts to minimize scattering from the positioning track to the receiver antenna.

E. Sources of Error in the Experiment

Great care was taken to minimize (but not necessarily remove) the primary sources of error in this experiment. These sources of remaining error are as follows.

- **Channel Transients**: Objects moving within the channel during the acquisition time of a PDP may distort the channel measurements. This effect is most pronounced outdoors, where even a slight breeze will rustle the leaves of trees and introduce small-but-noticeable fluctuations to all of the measured multipath components. In November, however, all of the deciduous trees had lost their leaves so this effect was largely absent from the data sets in this paper.
- **Self-Scattering Effects**: A large number of people and measurement equipment in the immediate area of the receiver may scatter multipath power to the receiver antenna that would be unrealistic. To remove this effect from each of the measurements, all personnel were evacuated from the immediate receiver area, the channel sounding hardware was kept as low to the ground as possible, and the receiver antenna was elevated above the positioning system so as to operate in an area of uncluttered free space.
- **Finite Sampling**: Due to finite sampling of PDP snapshots in a local area, all dispersion statistics derived from these measurements will be approximate. However, no single delay statistic presented in this paper was calculated from fewer than 36 PDP snapshots and no single angle-of-arrival statistic from fewer than 144 snapshots. The large number of snapshots per statistic produces reliable results. We have enough snapshots, in fact, to justify averaging channel statistics separately from the two track measurements within the same local area. With separate averages we can compare the similarities between the two track measurements, rather than assume isotropic statistics for all local areas.

III. Results

This section presents the delay dispersion, angle dispersion, and joint angle and delay statistics calculated from the measurement campaign. For a mathematical description and explanation of each channel parameter discussed, refer to Appendix A.

A. Delay Dispersion Results

Table I records all of the dispersion results for the 12 measured locations. This table records delay spread, centroid jitter, centroid standard deviation, timing jitter, and timing standard deviation for PDPs measured along orthogonal tracks.

For outdoor-to-outdoor links, the delay spreads in Table I range as low as 17 ns to as high as 219 ns. Low values for delay spread are found at location 4, the only line-of-sight link in the outdoor-to-outdoor measurements, as well as locations 5 and 6. It should be noted that the values in Table I are comparable to delay spreads measured by Patwari in [15] (from 25 to 333 ns), despite the increased average link distances. In fact, the correlation between delay spread and TR separation is weak. For example, the longest obstructed link—location 5 with 910 m of TR separation—has one of the smallest delay spreads at an average of 46 ns.

Delay spreads for indoor receivers demonstrate much more homogeneous behavior, independent of whether the transmitter is indoors or outdoors. The twelve indoor delay spreads (two for each track for locations 7–12) fall within a 27–45 ns range. Thus, a much simpler equalizer may be used if the radio is guaranteed to be operating indoors.

A final observation should be made about the variability of the delay spread about its mean value within a local area. The value *Timing Jitter* represents the difference between the smallest and largest delay spreads measured along a track. The value *Timing Standard Deviation* measures the mean-squared variation about the average delay spread in a local area. Both Timing Jitter and Timing Standard Deviation measure the variability of delay spread within a local area, but the Timing Standard Deviation may appear to be a better measure of typical behavior since it de-emphasizes the extreme cases of measured delay spread (see Appendix A).

B. Angle Dispersion Results

A number of other multipath parameters may also be calculated from the measured track and rotational data. Table II records transmitter-receiver separation distance, path loss with

TABLE I
SUMMARY OF DISPERSION STATISTICS CALCULATED FROM TRACK MEASUREMENTS

Location		x-axis					y-axis				
		Delay Spread	Centroid Jitter	Centroid Std. Dev.	Timing Jitter	Timing Std. Dev.	Delay Spread	Centroid Jitter	Centroid Std. Dev.	Timing Jitter	Timing Std. Dev.
1	OO	164 ns	118 ns	34 ns	128 ns	37 ns	138 ns	95 ns	22 ns	146 ns	30 ns
2	OO	196	89	22	90	20	148	101	23	101	26
3	OO	185	115	23	53	13	219	84	24	71	18
4	OO	55	17	4	24	6	22	15	4	20	5
5	OO	51	38	11	51	12	40	25	7	35	9
6	OO	25	8	2	16	4	17	6	2	10	3
7	II	30	33	8	13	4	29	26	6	18	4
8	II	45	29	5	24	6	45	29	7	20	5
9	II	44	40	11	25	6	42	31	8	25	6
10	OI	28	10	2	25	6	31	47	12	39	11
11	OI	35	37	10	46	10	44	46	12	44	12
12	OI	43	39	9	40	8	27	31	7	31	7
Average		75	48	12	44	11	67	45	11	47	11
Std. Dev.		62	36	9	32	9	62	30	7	39	8

OO – outdoor-to-outdoor II – indoor-to-indoor OI – outdoor-to-indoor

TABLE II
SUMMARY OF SPATIAL MULTIPATH PARAMETERS CALCULATED FROM SPATIALLY AVERAGED AZIMUTHAL SWEEPS OF A HORN ANTENNA

Location		Path Loss w.r.t. 1m FS	TR Sep Dist.	Angular Spread	Angular Constriction	Angle of Max. Fading	Peak Mult. Arrival
1	OO	90 dB	770 m	0.82	0.69	44°	0°
2	OO	51 dB	550 m	0.65	0.44	-63°	0°
3	OO	39 dB	240 m	0.91	0.51	36°	20°
4	OO	81 dB	585 m	0.52	0.77	89°	0°
5	OO	72 dB	910 m	0.46	0.70	76°	-10°
6	OO	83 dB	410 m	0.36	0.76	85°	0°
7	II	70 dB	29 m	0.73	0.52	84°	-10°
8	II	82 dB	33 m	0.74	0.50	30°	30°
9	II	76 dB	15 m	0.90	0.33	-74°	140°
10	OI	65 dB	340 m	0.78	0.72	85°	0°
11	OI	84 dB	365 m	0.86	0.19	-46°	10°
12	OI	85 dB	340 m	0.98	0.42	-38°	-50°
Average		73 dB	–	0.73	0.55	–	11°
Std. Dev.		15 dB	–	0.19	0.19	–	43°

OO – outdoor-to-outdoor II – indoor-to-indoor OI – outdoor-to-indoor

respect to 1-m free space (calculated from PDPs averaged linearly within a local area), the angular spread, and the peak multipath direction of arrival.

One trend that is apparent from Table II is the peak direction of multipath arrival. This parameter measures the direction in azimuth that the horn antenna was pointing when the maximum total power was received. According to Table II, the peak direction of multipath arrival is almost always in the direction of the transmitter (corresponding to 0°). This is true even for obstructed receiver locations. The one exception in Table II is location 9, where the peak direction of multipath arrival is 140°. However, location 9 is an indoor location corresponding to an indoor transmitter that is nearly directly above the receiver, with two floors in between. Given this unique location, the deviation from the trend is understandable. This property of the peak multipath arrival angle implies that an array scanning for peak power results in an effective direction-finding algorithm, even in heavily obstructed channels.

Another trend may be observed in the angular spread data. For indoor receivers at locations 7–12, the angular spread (the unitless metric defined in [8]) falls within the range 0.73–0.98. Thus, indoor angular spread values are almost always near the maximum value of 1.00. For outdoor receivers at locations 1–6, the angular spread falls within a range of lower values, 0.36–0.91. Thus, an omnidirectional multipath model for narrowband fading such as the Clarke model in [20] is not accurate for long-distance peer-to-peer links. The increase in angular spread indoors as opposed to outdoors may be explained by the increased density of scatterers (doors, walls, shelves, etc.) in all directions in an indoor environment.

Still another trend may be observed in the angular constriction data. From Table II, we see that the average value for an-

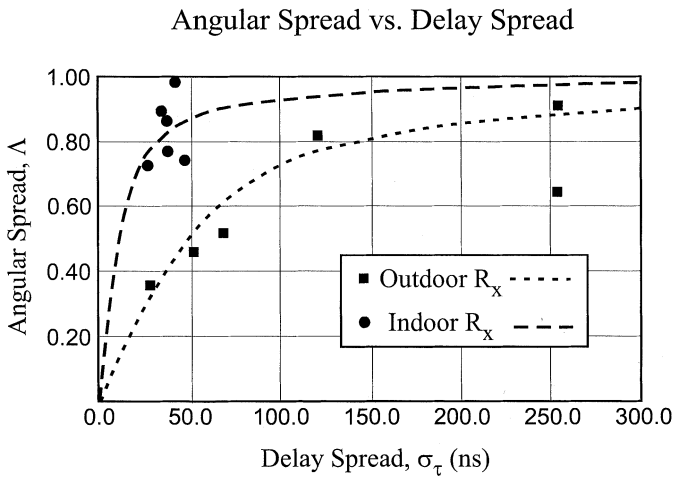

Fig. 6. Trend between angle spread and delay spread for indoor and outdoor receivers.

gular constriction γ is 0.55 (also unitless). This fairly large value indicates that multipath power is clustering about a few directions instead of being uniformly spread out in azimuth. This is another indication that idealized, uniform multipath models may not characterize the spatial fading behavior for the peer-to-peer channel.

C. Joint Angle-Delay Statistics

The graph in Fig. 6 shows angular spread vs. delay spread for the 12 measured local areas. We would expect that higher delay spreads indicate more multipath components from a larger variety of scattering mechanisms; under these circumstances, the angular spread should increase as well. While counterexamples certainly exist, most of the measured points in Fig. 6 follow this basic trend.

Note that the *rate* at which angular spread increases as a function of delay spread depends heavily on whether the receiver is indoors or outdoors. To study this effect quantitatively, we propose the following empirical guideline for angular spread, Λ, as a function of delay spread, σ_τ

$$\Lambda \approx \exp\left(-\frac{\sigma_c}{\sigma_\tau}\right). \tag{1}$$

The critical delay spread, σ_c, is the key parameter in (1) for determining the rate of angular spread increase. The critical delay spread may be calculated using linear regression on a set of measurement points, $(-\ln\Lambda,\ 1/\sigma_\tau)$. The six indoor points produce a critical delay spread value of 7.4 ns, while the six outdoor points produce a much larger σ_c of 32.5 ns. Plots of (1) for these two critical delay spreads are shown in Fig. 6.

IV. Conclusion

This paper presented a novel technique and quantitative results for measuring 1920 MHz peer-to-peer spatio-temporal radio channels. Angle and delay dispersion data were recorded for outdoor-to-outdoor, outdoor-to-indoor, and indoor-to-indoor transmitter-receiver configurations. This data set illuminates many of the following previously unmeasured, hypothetical trends in the peer-to-peer radio channel:

1) rms delay spread for outdoor-to-outdoor channel locations is an order of magnitude lower than PCS macrocellular radio channels, primarily due to the reduced transmitter antenna height.
2) rms delay spread for outdoor-to-indoor and indoor-to-indoor channels drops to around 35 ns—much lower than the outdoor-to-outdoor case.
3) Angular spread as measured at the receiver is higher for indoor receivers and lower for outdoor receivers.
4) A distinct, quantified trend shows how angular spread increases as delay spread increases.
5) Angular *constriction* is relatively high for all peer-to-peer channels, indicating that much of the multipath power is arriving from several discrete directions in azimuth instead of across a smooth continuum of azimuthal angles.

These quantified data trends will help engineers develop new spatio-temporal channel models and design wireless modems for radios operating in the peer-to-peer network configuration [21].

Appendix

V. Description of Measured Parameters

This appendix defines the terminology and parameters used in the analysis of the wideband, space-varying channels.

A. Noncoherent Channel Measurements

The wideband radio channel is measured as a function of space in this campaign using a *single-channel, noncoherent receiver*. Below is a list of terminology used to describe the types of channels measured during this campaign.

Channel Impulse Response (CIR): The CIR is the complex baseband representation of the radio channel $\tilde{h}(\tau, \vec{r})$. The CIR varies as a function of time-delay τ and vector position of receiver antenna in space $\vec{r}$. If a directional antenna is used at the receiver, the CIR may also depend on the azimuthal orientation of the antenna, θ.

Power Delay Profile (PDP): A noncoherent channel measures a PDP instead of a CIR. The PDP has units of *power* (related to physical units of *Watts* by a constant of proportionality) and is defined as the magnitude-squared of the CIR

$$p(\tau, \vec{r}) = \left|\tilde{h}(\tau, \vec{r})\right|^2. \tag{2}$$

Written without a θ-dependence, it may be assumed that (2) represents a measurement with an omnidirectional antenna.

Power Angle Profile (PAP): The PAP is the spatial equivalent of a PDP. The PAP has units of *power* and is defined as

$$p(\theta, \vec{r}) = \left|\tilde{h}(\theta, \vec{r})\right|^2. \tag{3}$$

Written without a τ-dependence, (3) represents the angle-of-arrival characteristics of a narrowband channel.

Angle-Delay Profile (ADP): When a directional antenna at position $\vec{r}$ and azimuthal orientation θ is connected to a wide-

band noncoherent channel sounder, an ADP is measured. The ADP has units of *power* and is defined as

$$p(\tau,\theta,\vec{r}) = \left|\tilde{h}(\tau,\theta,\vec{r})\right|^2. \tag{4}$$

B. Power Spectra

When power delay or angle profiles are linearly averaged in space, an estimate of a *power spectrum* is produced. Averaging various power profiles will produce the following normalized power spectra.

Delay Spectrum: Spatially averaging a collection of PDPs measured within the same local area produces an estimate for the delay spectrum $S_{\tilde{h}}(\tau)$ of the channel

$$S_{\tilde{h}}(\tau) \cong \frac{\sum_{i=1}^{N} p(\tau,\vec{r}_i)}{\int_{-\infty}^{+\infty}\left[\sum_{i=1}^{N} p(\tau,\vec{r}_i)\right]d\tau} \tag{5}$$

where $\{\vec{r}_i\}$ is the set of measurement positions. The delay spectrum characterizes the frequency selectivity of the stochastic, time-varying radio channel [22].

Angle Spectrum: Spatially averaging a collection of PAPs measured within the same local area produces an estimate for the angle spectrum $S_{\tilde{h}}(\theta)$ of the channel

$$S_{\tilde{h}}(\theta) \cong \frac{\sum_{i=1}^{N} p(\theta,\vec{r}_i)}{\int_{-\infty}^{+\infty}\left[\sum_{i=1}^{N} p(\theta,\vec{r}_i)\right]d\theta}. \tag{6}$$

The angle spectrum characterizes the spatial selectivity of the stochastic, space-varying radio channel [8], [23].

Angle-Delay Spectrum (ADS): Spatially averaging a set of full ADPs within the same local area produces an estimate for the joint ADS, $S_{\tilde{h}}(\tau,\theta)$

$$S_{\tilde{h}}(\tau,\theta) \cong \frac{\sum_{i=1}^{N} p(\tau,\theta,\vec{r}_i)}{\int_{-\infty}^{+\infty}\int_{-\infty}^{+\infty}\left[\sum_{i=1}^{N} p(\tau,\theta,\vec{r}_i)\right]d\theta d\tau}. \tag{7}$$

This joint power spectrum characterizes the full spatio-temporal randomness of the radio channel.

Note, that the use of power spectra in channel modeling assumes radio channels are wide-sense stationary in space and frequency over basic intervals of interest. The frequency interval of interest is the *RF bandwidth* of the transmitted signal and the spatial interval of interest is the *local area*. Definitions for the coherence bandwidth and the coherence distance of a fading radio channel are based on delay and angle spectra, respectively.

C. Time Delay Parameters

A number of delay dispersion parameters are measured in this campaign and reported in this paper. Each parameter is calculated for a measured local area and is defined below. Note that before each statistic is calculated, all power at or below the noise + interference floor of the received profile is zeroed.

Centroid, $\bar{\tau}$: The centroid is the *first moment* of a delay spectrum. The nth moment of a spectrum is defined as

$$\overline{\tau^n} = \frac{\int_{-\infty}^{+\infty}\tau^n S_{\tilde{h}}(\tau)d\tau}{\int_{-\infty}^{+\infty} S_{\tilde{h}}(\tau)d\tau}. \tag{8}$$

Thus, the centroid is (8) evaluated for $n = 1$.

rms Delay Spread, σ_τ: The rms delay spread is the *second centered moment* of a delay spectrum, defined mathematically as

$$\sigma_\tau = \sqrt{\overline{\tau^2} - (\overline{\tau})^2}. \tag{9}$$

The rms delay spread is related to the frequency selectivity of a wideband multipath channel [24].

Centroid Jitter: If the centroid were calculated from a single PDP instead of the delay spectrum using the definition in (8), then each local area would have a set of centroids as a function of space, $\{\overline{\tau}(\vec{r}_i)\}$. The *centroid jitter* is the maximum centroid value minus the minimum centroid value measured in the same local area. This value measures range of possible centroid fluctuations within a local area.

Centroid Standard Deviation: This measure is defined similar to centroid jitter except it is the standard deviation of the set of centroids, $\{\overline{\tau}(\vec{r}_i)\}$, measured within the same local area. This measure is less sensitive to pathological instances of centroid measured at one or two points.

Timing Jitter: This parameter, defined by Devasirvatham in [25], is based on the set of instantaneous rms delay spreads, $\{\sigma_\tau(\vec{r}_i)\}$, calculated from PDPs in a local area. The timing jitter is the maximum delay spread minus the minimum delay spread measured in the same local area. This value measures the range of possible rms delay spread fluctuations within a local area.

Timing Standard Deviation: This measure is defined similar to timing jitter except it is the standard deviation of the set of rms delay spreads, $\{\sigma_\tau(\vec{r}_i)\}$, measured within the same local area. This measure is less sensitive to pathological instances of rms delay spread measured at one or two points.

D. Angle-of-Arrival Parameters

There are also several angular dispersion parameters that are measured in this campaign and reported in this paper. Each parameter is also calculated for a measured local area and defined below:

Peak Angle of Arrival, θ_{peak}: This parameter, calculated from the estimate of angle spectrum $S_{\tilde{h}}(\theta)$, is the azimuthal angle in which the largest average multipath power is received.

Angular Spread, Λ: This parameter ranges between 0 and 1 and describes how multipath power concentrates about a single direction-of-arrival in space, with 0 denoting perfect concentration in one direction and 1 representing no clear directional bias in arriving multipath power. The angular spread is calculated from complex Fourier coefficients of the angle spectrum

$$F_n = \int_0^{2\pi} S_{\tilde{h}}(\theta)\exp(jn\theta)d\theta \tag{10}$$

and is mathematically defined as [1]

$$\Lambda = \sqrt{1 - \frac{|F_1|^2}{F_0^2}}. \tag{11}$$

This definition of angular spread is directly related to spatial selectivity in a narrowband multipath channel: larger values of angular spread imply more spatial selectivity.

Angular Constriction, γ: This parameter also ranges between 0 and 1 and describes how multipath power concentrates about two directions-of-arrival in space, with 1 denoting perfect concentration in two directions and 0 representing no clear bias in two directions. The angular constriction is mathematically defined as

$$\gamma = \frac{\left|F_2 F_0 - F_1^2\right|}{F_0^2 - |F_1|^2}. \tag{12}$$

Angular constriction is also directly related to spatial selectivity in a narrowband multipath channel: larger values of angular constriction imply spatial selectivity in a local area that is *anisotropic*, depending on the orientation of movement in space.

Angle of Maximum Fading, $\theta_{\max}$: This parameter represents the azimuthal direction in space that a receiver must move to experience the maximum possible spatial selectivity. It is defined to be

$$\theta_{\max} = \frac{1}{2} \arg\left(F_2 F_0 - F_1^2\right). \tag{13}$$

ACKNOWLEDGMENT

The authors would like to thank J. Siew, E. Lau, C. Steger, P. Cardieri, J. Aron, and B. Puckett for their assistance in measured data collection and processing. They also thank Dr. J. Isaacs of ITT Defense and Electronics for his support and encouragement of this work.

REFERENCES

[1] G. D. Durgin and T. S. Rappaport, "A basic relationship between multipath angular spread and narrowband fading in a wireless channel," *IEE Electron. Lett.*, vol. 34, no. 25, pp. 2431–2432, Dec. 10, 1998.

[2] Y. Wu and W. Y. Zou, "Orthogonal frequency division multiplexing: a multicarrier modulation scheme," *IEEE Trans. Consumer Electron.*, vol. 41, pp. 392–399, Aug. 1995.

[3] L. C. Godara, "Applications of antenna arrays to mobile communications, part I: performance improvement, feasibility, and system considerations," *Proc. IEEE*, vol. 85, no. 7, pp. 1031–1060, July 1997.

[4] G. J. Foschini, "Layered space-time architecture for wireless communication in a fading environment when using multi-element antennas," *Bell Labs Tech. J.*, pp. 41–59, Autumn 1996.

[5] A. R. Calderbank, G. Pottie, and N. Seshadri, "Cochannel interference suppression through time/space diversity," *IEEE Trans. Inform. Theory*, vol. 46, pp. 922–932, May 2000.

[6] P. C. F. Eggers, "Angular dispersive mobile radio environments sensed by highly directive base station antennas," in *Proc. PIMRC '95*, Toronto, Canada, Sept. 1995, pp. 522–526.

[7] Q. H. Spencer, B. D. Jeffs, M. A. Jensen, and A. L. Swindlehurst, "Modeling the statistical time and angle of arrival characteristics of an indoor multipath channel," *IEEE J. Select. Areas Commun.*, vol. 18, pp. 347–360, Mar. 2000.

[8] G. D. Durgin and T. S. Rappaport, "Theory of multipath shape factors for small-scale fading wireless channels," *IEEE Trans. Antennas Propagat.*, vol. 48, pp. 682–693, May 2000.

[9] F. Ikegami and S. Yoshida, "Analysis of multipath propagation structure in urban mobile radio environments," *IEEE Trans. Antennas Propagat.*, vol. 28, pp. 531–537, July 1980.

[10] J. Fuhi, J.-P. Rossi, and E. Bonek, "High-resolution 3-D direction-of-arrival determination for urban mobile radio," *IEEE Trans. Antennas Propagat.*, vol. 45, pp. 672–682, Apr. 1997.

[11] J.-P. Rossi, J.-P. Barbot, and A. J. Levy, "Theory and measurement of the angle of arrival and time delay of UHF radiowaves using a ring array," *IEEE Trans. Antennas Propagat.*, vol. 45, pp. 876–884, May 1997.

[12] K. I. Pedersen, P. E. Mogensen, and B. H. Fleury, "A stochastic model of the temporal and azimuthal dispersion seen at the base station in outdoor propagation environments," *IEEE Trans. Veh. Technol.*, vol. 49, pp. 437–447, Mar. 2000.

[13] S. Y. Seidel, T. S. Rappaport, S. Jain, M. L. Lord, and R. Singh, "Path loss, scattering, and multipath delay statistics in four European cities for digital cellular and microcellular radiotelephone," *IEEE Trans. Veh. Technol.*, vol. 40, no. 4, pp. 721–730, Nov. 1991.

[14] M. J. Feuerstein, K. L. Blackard, T. S. Rappaport, S. Y. Seidel, and H. H. Xia, "Path loss, delay spread, and outage models as functions of antenna height for microcellular system design," *IEEE Trans. Antennas Propagat.*, vol. 43, pp. 487–498, Aug. 1994.

[15] N. Patwari, G. D. Durgin, T. S. Rappaport, and R. J. Boyle, "Peer-to-peer low antenna outdoor radio wave propagation at 1.8 GHz," in *Proc. IEEE 49th Vehicular Technology Conf.*, vol. 1, Houston, TX, May 1999, pp. 371–375.

[16] V. Erceg, D. G. Michelson, S. S. Ghassemzadeh, L. J. Greenstein, A. J. Rustako Jr., P. B. Guerlain, M. K. Denuison, R. S. Roman, D. J. Barnickel, S. C. Wang, and R. R. Miller, "A model for the multipath delay profile of fixed wireless channels," *IEEE J. Select. Areas Commun.*, vol. 17, pp. 399–410, Mar. 1999.

[17] D. M. J. Devasirvatham, R. R. Murray, and C. Banerjee, "Time delay spread measurements at 850 MHz and 1.7 GHz inside a metropolitan office building," *IEE Electron. Lett.*, vol. 25, no. 3, pp. 194–196, Feb. 2, 1989.

[18] G. Woodward, I. Oppermann, and J. Talvitie, "Outdoor-indoor temporal and spatial wideband channel model for ISM bands," in *Proc. IEEE 49th Vehicular Technology Conf.*, Houston, TX, May 1999, pp. 136–140.

[19] W. G. Newhall, K. Saldanha, and T. S. Rappaport, "Using RF channel sounding measurements to determine delay spread and path loss," *R. F. Des.*, pp. 82–88, Jan. 1996.

[20] R. H. Clarke, "A statistical theory of mobile-radio reception," *Bell Syst. Tech. J.*, vol. 47, pp. 957–1000, 1968.

[21] G. D. Durgin, *Space-Time Wireless Channels*. Englewood Cliffs, NJ: Prentice-Hall, 2002.

[22] G. D. Durgin and T. S. Rappaport, "Spatial channel modeling for wireless communications," in *Wireless Communications for the New Milleniurn*, N. Morinaga, R. Kohno, and S. Sampei, Eds. Boston, MA: Kluwer, 2000.

[23] M. J. Gans, "A power-spectral theory of propagation in the mobile radio environment," *IEEE Trans. Veh. Technol.*, vol. VT-21, pp. 27–38, Feb. 1972.

[24] J. C.-I. Chuang, "The effects of time delay spread on portable radio communications channels with digital modulation," *IEEE J. Select. Areas Commun.*, vol. SAC-5, pp. 879–889, June 1987.

[25] D. M. J. Devasirvatham, "A comparison of time delay spread and signal level measurements within two dissimilar office buildings," *IEEE Trans. Antennas Propagat.*, vol. AP-35, pp. 319–324, Mar. 1987.

Gregory D. Durgin (S'98–M'00) was born in Baltimore, MD, on October 23, 1974. He received the B.S.E.E., M.S.E.E., and Ph.D. degrees from Virginia Polytechnic Institute and State University (Virginia Tech), Blacksburg, in 1996, 1998, and 2000, respectively.

He performed his graduate work at the Mobile and Portable Radio Research Group (MPRG), Virginia Tech, where he was a highly ranked course Instructor and performed research in electron optics, fluorescent microscopy and holography, robotics, propagation, and RF engineering. From 2001 to 2002, he served as a Postdoctoral Fellow from the Japanese Society for the Promotion of Science (JSPS) at Morinaga Laboratory, Osaka University, Osaka, Japan, where he performed research in space-time channel modeling. He also serves regularly as a consultant to industry. He is the author and coauthor of numerous international journal/conference papers and two books, including the textbook *Space-Time Wireless Channels* (Engelwood Cliffs, NJ: Prentice-Hall, 2002). His current research areas include antennas and propagation, wireless LANs, and engineering education.

Dr. Durgin received the Blackwell Award for best graduate research presentation in the Electrical and Computer Engineering Department, Virginia Tech, and was a corecipient for the Stephen O. Rice Prize for Best Original Research Paper published in the IEEE TRANSACTIONS ON COMMUNICATIONS, both in 1998.

Vikas Kukshya received the the B.E. degree in electronics and communications engineering (where he graduated at the top of his class) from Gujarat University, Gujarat, India, in 1997 and the M.S.E.E. degree from Virginia Polytechnic Institute and State University (Virginia Tech), Blacksburg, in June 2001.

Prior to his undergraduate degree, he was an Engineer Trainee at Space Applications Center (SAC), Indian Space Research Organization (ISRO), where he was responsible for the development and evaluation of a single board computer (SBC) for the 'OCEANSAT' satellite system. In 1997, he joined Tata Telecom Limited, New Delhi, India—a joint venture company of Tata and Lucent Technologies, as an Engineer specializing in telecommunications. In 1999, he joined Virginia Tech to pursue his M.S.E.E. degree and worked as a Research Assistant at Mobile and Portable Radio Research Group (MPRG) under the guidance of Dr. Theodore S. Rappaport. At MPRG, he specialized in wideband propagation measurements, and channel modeling at millimeter wave frequencies for pico-cell scenarios. In 2001, he joined HRL Laboratories, Malibu, CA—the corporate research and development facility of Boeing, General Motors, and Raytheon. At HRL Laboratories, he has been actively working on free-space laser optics technology, broadband wireless access systems, and software radios.

Mr. Kukshya was awarded three university gold medals for academic excellence from Gujarat University and Certificates of Merit by the Vice President and Managing Director of Tata Telecom Limited.

Theodore S. Rappaport (S'83–M'83–SM'90–F'98) received the B.S.E.E., M.S.E.E., and Ph.D. degrees from Purdue University, West Lafayette, IN, in 1982, 1984, and 1987, respectively.

From 1988 to 2002, he was a faculty member in the Electrical and Computer Engineering Department, Virginia Polytechnic Institute and State University (Virginia Tech), Blacksburg, where he was the James S. Tucker Professor and founder of the Mobile and Portable Radio Research Group (MPRG), one of the world's first university research and teaching centers dedicated to the wireless communications field. In 1989, he founded TSR Technologies, Incorporated, a cellular radio/PCS manufacturing firm that he sold in 1993. He formed Wireless Valley Communications, Incorporated, in 1995 and relocated the company to Austin, TX, in 2002. He recently joined the University of Texas (UT), Austin, as the William and Bettye Nowlin Chair in Electrical Engineering and is director of the newly formed Wireless Networking and Communications Group on UT's Austin campus. He has consulted for over 25 multinational corporations and has served the International Telecommunications Union as a consultant for emerging nations. He also serves as Chairman of Wireless Valley Communications, Incorporated, an in-building/campus design and management product company. He has 28 patents issued or pending and has authored, coauthored, and coedited 18 books in the wireless field, including the textbooks *Wireless Communications: Principles & Practice* (Englewood Cliffs, NJ: Prentice-Hall, 1996, 2002), *Smart Antennas for Wireless Communications: IS-95 and Third Generation CDMA Applications* (Englewood Cliffs, NJ: Prentice-Hall, 1999). He has coauthored more than 200 technical journal and conference papers. Since 1998, he has been Series Editor for the *Prentice-Hall Communications Engineering and Emerging Technologies Book Series*. He serves on the Editorial Board of the *International Journal of Wireless Information Networks* and the Advisory Board of *Wireless Communications and Mobile Computing*.

Dr. Rappaport is a Registered Professional Engineer in the state of Virginia. He received the Marconi Young Scientist Award in 1990, a National Science Foundation (NSF) Presidential Faculty Fellowship in 1992, and the James R. Evans Avante Garde award from the IEEE Vehicular Technology Society in 2002. He is active in the IEEE Communications and Vehicular Technology Societies and is a Fellow and Past Member of the Board of Directors of the Radio Club of America.